Carbohydrate Polymers 100 (2014) 211–217

Contents lists available at ScienceDirect

Carbohydrate Polymers

journal homepage: www.elsevier.com/locate/carbpol

# Effect of [Emim]Ac pretreatment on the structure and enzymatic hydrolysis of sugarcane bagasse cellulose

Jing Bian[a], Feng Peng[a,b], Xiao-Peng Peng[c], Xiao Xiao[d], Pai Peng[b], Feng Xu[a], Run-Cang Sun[a,b,*]

[a] Beijing Key Laboratory of Lignocellulosic Chemistry, Beijing Forestry University, Beijing 100083, China
[b] State Key Laboratory of Pulp and Paper Engineering, South China University of Technology, Guangzhou 510640, China
[c] State Key Laboratory of Tree Genetics and Breeding, Chinese Academy of Forestry, Beijing 100091, China
[d] College of Science, Northwest A&F University, Yangling 712100, China

ARTICLE INFO

*Article history:*
Received 25 July 2012
Received in revised form 10 October 2012
Accepted 26 February 2013
Available online 5 March 2013

*Keywords:*
Cellulose
Ionic liquid
Crystallinity
Enzymatic hydrolysis

ABSTRACT

Effect of ionic liquid pretreatment on enzymatic hydrolysis of cellulose was investigated in terms of the changes in the chemical and physical structure of the preparation. In this case, original cellulose isolated from sugarcane bagasse was subjected to ionic liquid ([Emim]Ac) dissolution at a mild temperature (90 °C) followed by regeneration in water and subsequently hydrolyzed by commercial cellulases. The original and regenerated cellulose were thoroughly characterized by XRD, FT-IR, CP/MAS $^{13}$C NMR, and SEM. It was found that the original cellulose experienced an increase in glucose content from 80.0–83.3% to 91.6–92.8%, a decrease in the degree of polymerization from 974–1039 to 511–521, a crystal transformation from cellulose I to cellulose II, as well as an increase of surface area during the pretreatment. The results suggested that pretreatment led to effective disruption of cellulose for subsequent enzyme hydrolysis as evidenced by a high glucose conversion yield of 95.2%.



## 1. Introduction

The rapid consumption of fossil fuel resources has motivated researchers to pursue renewable and sustainable sources (Farrell et al., 2006). Lignocellulosic biomass has been recognized as a potential renewable feedstock for bioconversion into biofuels and value-added chemicals (Lee, Doherty, Linhardt, & Dordick, 2009; Richard, 2010). Lignocelluloses are mainly composed of cellulose, hemicelluloses and lignin. Among them, cellulose is the most abundant component and has a great potential in the conversion into bio-fuels, chemicals and materials (Pandey et al., 2000). It is a linear homopolymer of $\beta$-(1 → 4)-linked glucopyranose repeating units, consisting of amorphous and highly structured crystalline regions (Pinkert, Marsh, Pang, & Staiger, 2009). The crystalline structure of native cellulose fibers, called cellulose I, consists of parallel chains align side-by-side via hydrogen bonding in flat sheets (Nishiyama, Sugiyama, Chanzy, & Langan, 2003). After mercerization or regeneration, cellulose I is transformed into cellulose II. Cellulose II comprises a two-chain monoclinic unit cell in which the cellulose chains are stacked with opposite polarity, in an antiparallel chain packing (Wada, Ike, & Tokuyasu, 2010).

Due to the stiffness of the molecule and the close packing of the chains via numerous intermolecular and intramolecular hydrogen bonds (Azubuike, Rodríguez, Okhamafe, & Rogers, 2011), cellulose is difficult to dissolve in conventional solvents and to hydrolyze into fermentable sugars (Arantes & Saddler, 2011). Therefore, pretreatment is a necessary step to disrupt the tight packing arrangement of cellulose fibrils in the crystalline domains, for enhancing enzymes accessibility to cellulose during hydrolysis. Dissolution of cellulose by cellulose solvents is considered as one of the easiest methods for disrupting cellulose structure. Generally, cellulose solvents can be divided into derivative solvents and non-derivative solvents. The derivative solvents dissolve cellulose by conversion of the cellulose into a soluble transient derivative or intermediate, whereas the non-derivative solvents dissolve cellulose by disrupting the hydrogen bonds without the formation of a derivative (Liebert, 2010). In order to improve the reactivity of cellulose, numerous non-derivative solvents, such as N-methyl-morpholine-N-oxide (NMMO), concentrated phosphoric acid, and ionic liquids (ILs), have been used to pretreat cellulose for enzymatic hydrolysis (Kuo & Lee, 2009). Among them, ILs have recently emerged as promising non-derivative solvents for the dissolution of lignocelluloses. It has been reported that 1-allyl-3-methylimidazolium-chloride ([Amim]Cl) is the most effective ionic liquid for dissolving wood

* Corresponding author at: Beijing Key Laboratory of Lignocellulosic Chemistry, Beijing Forestry University, Beijing 100083, China. Tel.: +86 1062336903; fax: +86 1062336903.
*E-mail address:* rcsun3@bjfu.edu.cn (R.-C. Sun).

0144-8617/$ – see front matter © 2013 Elsevier Ltd. All rights reserved.
http://dx.doi.org/10.1016/j.carbpol.2013.02.059

chips, and 1-ethyl-3-methylimidazolium-acetate ([Emim]Ac) has good dissolving capability for cellulose (Zavrel, Bross, Funke, Büchs, & Spiess, 2009). Overall, extensive effort has been devoted to direct dissolution of lignocellulosic material and separation of the constitutive major biopolymers. However, a clear separation of cellulose can not be attained from the direct dissolving process (Azubuike et al., 2011). After the IL pretreatment of the feedstock, the cellulose in the raw material is much more prone to degradation by cellulase (Dadi, Schall, & Varanasi, 2007). However, with respect to the investigation on the cellulose, the starting materials adopted in many studies are commercial products, such as Avicel and cotton, which have different properties from the cellulose in natural lignocellulosic biomass.

Up to now, there is a little information available on the chemical and physical changes of cellulose after IL pretreatment and their impact on the subsequent hydrolysis. As a consequence, the current research is specifically focused on this aspect. In this study, cellulose was isolated from sugarcane bagasse, a typical agricultural lignocellulosic material, and subsequently pretreated with ionic liquid [Emim]Ac. Enzymatic hydrolysis of the ionic liquid pretreated cellulose and the original cellulose was compared to investigate the correlation between changes in cellulose structure and digestibility. The chemical and physical changes between the original and reconstituted cellulose were thoroughly characterized by X-ray diffraction (XRD), Fourier transform infrared spectroscopy (FT-IR), solid polarized/magic angle spinning (CP/MAS) $^{13}C$ NMR, and scanning electron microscopy (SEM). The intrinsic viscosity and molecular weight of the original and regenerated cellulose were also determined. The relationship between the structural changes and the enzymatic hydrolysis allow us to better understand the mechanism involved in the enzymatic hydrolysis resulting from IL [Emim]Ac pretreatment and to further improve the efficiency of the process.

## 2. Experimental

### 2.1. Materials

Sugarcane bagasse was collected in a sugar factory (Guangzhou, China). It was air dried, milled, screened to obtain the particles of 40–80 mesh, and then stored until used. The ionic liquid [Emim]Ac (≥98.5%) was purchased from Lanzhou Institute of Chemical Physics, Lanzhou, China. Celluclast 1.5 L (cellulase) and Novozyme 188 (β-glucosidase) were provided by Novozymes (China) Investment Co. Ltd.

### 2.2. Isolation of cellulose from sugarcane bagasse

The dried sugarcane bagasse powder was first delignified with sodium chlorite in acidic solution (pH 3.8–4.0, adjusted by acetic acid) at 75 °C for 2 h. The holocellulose was then extracted with 10% KOH to remove hemicelluloses with a solid to liquor ratio of 1:20 (g ml$^{-1}$) for 10 h at 20 °C, 30 °C, 40 °C, and 50 °C, respectively. The remaining solids, considered to be original cellulose, were filtrated and washed thoroughly with water until the filtrate was neutral, and dried in an oven at 55 °C for 16 h.

### 2.3. Cellulose dissolution and regeneration

Ionic liquid [Emim]Ac (10.0 g) was added to a dried flask containing 0.3 g of the original cellulose. The mixture was then placed into an oil bath heated to 90 °C and the dissolution proceeded with vigorous magnetic stirring (700 rpm) for 6 h, under an inert atmosphere of nitrogen. After the reaction, distilled water was poured into the flask under stirring, and the precipitates were recovered as regenerated cellulose. The resulting precipitates were washed with distilled water at 60 °C several times to remove IL and then freeze-dried. The cellulose preparations were considered to be regenerated cellulose IL20, IL30, IL40, and IL50, respectively, according to the corresponding crude cellulose. The scheme for the treatment process of sugarcane bagasse is illustrated in Fig. 1.

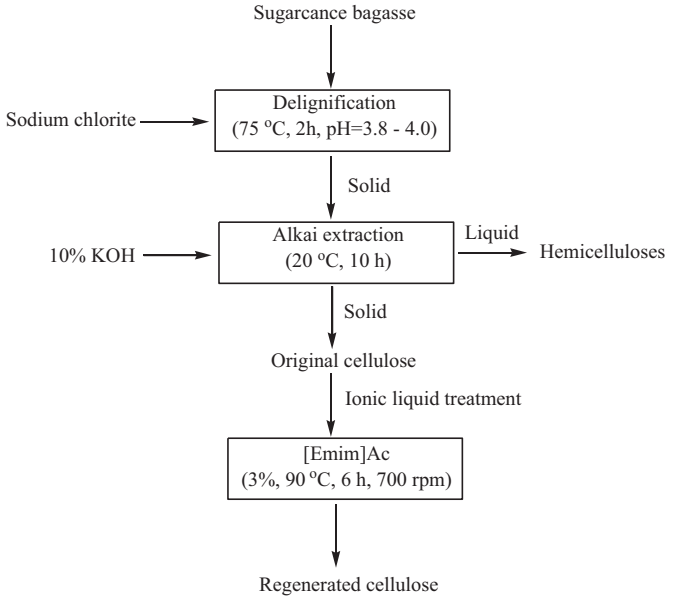


**Fig. 1.** Schematic illustration of the experimental procedure.

### 2.4. Enzymatic hydrolysis of cellulose samples

Enzymatic hydrolysis was performed at 50 °C in 0.05 M citrate buffer (pH 4.8) with 2% original and regenerated cellulose substrate in a 25 ml conical flask. The enzyme loadings were 35 FPU/g (cellulase) and 40 CbU (β-glucosidase) in relation to the dry weight of cellulose substrates. Samples were periodically withdrawn, and glucose concentration was determined by a HPAEC system. All reactions were carried out in triplicate.

### 2.5. Analysis methods

The viscosity-average degree of polymerization ($P$) of the cellulose preparations was determined by the cupri-ethylene-diamine (CED) method as described elsewhere (Wang, Jiang, Xu, & Sun, 2009) and calculated using the following equation:

$$P^{0.90} = \frac{1.65\,[\eta]}{\text{ml g}^{-1}} \quad (1)$$

The molecular weight of the cellulose was then calculated, using $P$ multiplying by 162, the molecular weight of an anhydroglucose.

The carbohydrate compositions of the original and regenerated cellulose preparations were analyzed by high-performance anion exchange chromatography (HPAEC) (Dionex, ICS 3000, USA) equipped with a CarboPac PA 20 analytical column and an amperometric detector. The glucose yield was calculated as follows:

$$\text{Glucose yield (\%)} = \frac{\text{Released glucose weight} \times 0.9}{\text{Cellulose substrate weight} \times \text{content of glucose}} \times 100 \quad (2)$$

The X-ray powder diffraction pattern of the original and regenerated cellulose preparations was measured using an XRD-6000 instrument (Shimadzu, Japan) with a Cu Kα radiation source (λ = 0.154 nm) at 40 kV and 30 mA. Samples were scanned from

$2\theta = 5–50^\circ$ at a speed of $2^\circ$/min. The crystallinity, as expressed by the crystallinity index (*CrI*), was determined by the Segal method (Segal, Creely, Martin Jr, & Conrad, 1959). The following empirical equation was adopted to estimate the crystallinity index:

$$CrI\,(\%) = 100 \times \frac{I_{total} - I_{am}}{I_{total}} \quad (3)$$

In which $I_{total}$ is the scattered intensity at the main peak, whereas $I_{am}$ is the scattered intensity due to the amorphous portion (Cheng et al., 2011).

Fourier transform infrared (FT-IR) spectra were recorded using a Nicolet iN10 FT-IR microscope (Thermo Nicolet Corporation, Madison, WI) equipped with a liquid nitrogen-cooled MCT detector. The spectra collected were the average of 64 scans recorded at a resolution of 8 $cm^{-1}$ in the range of 4000–750 $cm^{-1}$.

CP/MAS $^{13}C$ NMR spectra of the samples were obtained at 100 MHz using a Bruker AV-III 400 M spectrometer (Germany). Cellulose samples were packed in 4 mm zirconia ($ZrO_2$) rotors, and the measurements were performed using a CP pulse program with 1 ms match time and a 2 s delay between transients. The spinning rate was 5 kHz.

Scanning electron microscopy of the original and regenerated cellulose samples was carried out with a Hitachi S-3400 N II (Hitachi, Japan) instrument at 15 kV. Before the determination, samples were mounted with conductive glue and coated with a thin layer of gold to improve the conductivity and the quality of the SEM images.

## 3. Results and discussion

### 3.1. Dissolution and regeneration of cellulose

In the plant cell wall, cellulose, hemicelluloses and lignin are closely associated with each other. Hemicelluloses are integrated into the structure of cellulose, and locate within and between cellulose fibrils (Duchesne et al., 2001). Lignin is covalently bound to hemicelluloses and cross-linked to cellulose microfibrils. The complicated structure of lignocelluloses reduces the reactivity of cellulose towards digestion. In the present study, to better evaluate the changes in cellulose after the pretreatment on its digestibility, cellulose in the lignocellulose was firstly isolated by delignification and hemicelluloses removal. After that, the cellulose obtained, denoted as original cellulose, was subjected to sugar composition analysis by HPAEC, since chemical composition determination constitutes the first step in characterization of the lignocelluloses for biofuel production and in determining the changes imparted by pretreatment (Cateto, Hu, & Ragauskas, 2011). The features of the original cellulose can be found in our previous study (Bian et al., 2012). It was found that a large amount of xylose (~13–18%) and minor quantities of arabinose, galactose, and uronic acids were detected in the original cellulose samples. This indicated that the original cellulose obtained indeed contained a noticeable amount of hemicelluloses which may be the relatively resistant part in the material. Ionic liquid [Emim]Ac was used to dissolve the original cellulose samples at a low temperature of 90 °C. It should be noted that higher temperatures facilitate the dissolution, but result in more degradation of cellulose (Sun et al., 2009). After precipitation into water, the cellulose samples, denoted as regenerated cellulose, was recovered. The data of sugar analysis of the regenerated cellulose are given in Table 1. The regenerated cellulose contained relatively lower content of xylose (7.3–8.0%), arabinose (0.3%), and galactose (0.1%) as compared to the original cellulose. Decrease in content of the sugars after IL pretreatment suggested that part of resistant hemicelluloses were solubilized into the IL. The pretreatment with ionic liquid led to higher levels of glucose in the samples, ranged between 91.6 and 92.8%, as compared to 80.0 and 83.3% in the original cellulose. This was in good agreement with the report by Lee et al. (2009), who has found that [Emim]Ac treatment removed 26% hemicelluloses from wood flour.

**Table 1**
Sugar composition of the regenerated cellulose preparations obtained by pretreating the original cellulose samples with [Emim]Ac from sugarcane bagasse (all the values represent mean values from duplicate experiments, with 5–10% standard error).

| Cellulose[a] | Arabinose | Galatose | Glucose | Xylose | Uronic acid |
|---|---|---|---|---|---|
| IL20 | 0.3 | 0.1 | 92.0 | 7.6 | ND[b] |
| IL30 | 0.3 | 0.1 | 92.8 | 6.7 | ND[b] |
| IL40 | 0.3 | 0.1 | 91.6 | 8.0 | ND[b] |
| IL50 | 0.3 | 0.1 | 92.3 | 7.3 | ND[b] |

[a] Corresponding to the regenerated cellulose preparations.
[b] Not detected.

Degree of polymerization has been considered as an important factor in determining the hydrolysis rates of cellulosic substrates (Chang & Holtzapple, 2000). Table 2 gives the intrinsic viscosity ($\eta$), viscosity average degree of polymerization ($P$), and molecular weight ($M_w$) of the regenerated cellulose. As compared to the degree of polymerization ($P$, 974–1039) and the molecular weight ($M_w$, 157 800–168 370 g/mol) of the original cellulose, the degree of polymerization and $M_w$ of the regenerated cellulose samples obtained were much lower ($P$, 511–521; $M_w$, 82 780–84 400 g/mol). This indicated that the ionic liquid pretreatment depolymerizes cellulose to some extent.

### 3.2. X-ray diffraction

The diffractograms of the original cellulose exhibit diffraction typical of cellulose I, with diffractogram peaks of $2\theta$ at 15.4°, 16.2° and 22.7°. The peaks of $2\theta$ at 15.4° and 16.2° are the overlapping signals of $1\,\bar{1}\,0$ and $1\,1\,0$ reflections, and 22.7° can be assigned to $2\,0\,0$ reflections (Zuluaga et al., 2009). The X-ray diffractograms of all four regenerated cellulose preparations are shown in Fig. 2. The diffractograms exhibit a different pattern as compared to the original cellulose. The main peak at 22.7° present in the original cellulose disappeared, and a broad peak consisting of a doublet at 20.1° and 21.7° appeared. The peak at 16.2° is largely weakened and shifted to 12.2°. These changes confirmed that the treatment with ionic liquid [Emim]Ac involved dissolution and regeneration where the native crystalline structure was disrupted and transformed to cellulose II upon precipitation into water (Sun et al., 2009). It has been reported that the transformation processes were distinctly different for Avicel and lignified samples treated with ILs, due to the presence of lignin in the lignified samples interfering with cellulose I dissolution and structuring (Cheng et al., 2011). For Avicel, a crystal transformation to cellulose II occurred, and for lignified samples, the IL pretreatment resulted in an expansion of cellulose I lattice. The change in cellulose crystal in the present study is in accordance with the observation from studies on Avicel where the dissolved cellulose chains solvated in IL crystallize into cellulose II. Cellulose II is a more thermodynamically stable crystalline form

**Table 2**
Intrinsic viscosity ($\eta$), viscosity average DP ($P$), and molecular weight ($M_w$) of the regenerated cellulose preparations from ionic liquid.

| Cellulose sample[a] | $\eta$ | $P$ | $M_w$ |
|---|---|---|---|
| IL20 | 169 | 521 | $8.44 \times 10^4$ |
| IL30 | 166 | 511 | $8.28 \times 10^4$ |
| IL40 | 166 | 511 | $8.28 \times 10^4$ |
| IL50 | 167 | 514 | $8.33 \times 10^4$ |

[a] IL20, IL30, IL30, IL40, and IL50 represent the regenerated cellulose preparations obtained by [Emim]Ac pretreatment of the original cellulose samples isolated by 10% KOH at 20, 30, 40, and 50 °C for 10 h, respectively, from sugarcane bagasse holocellulose.

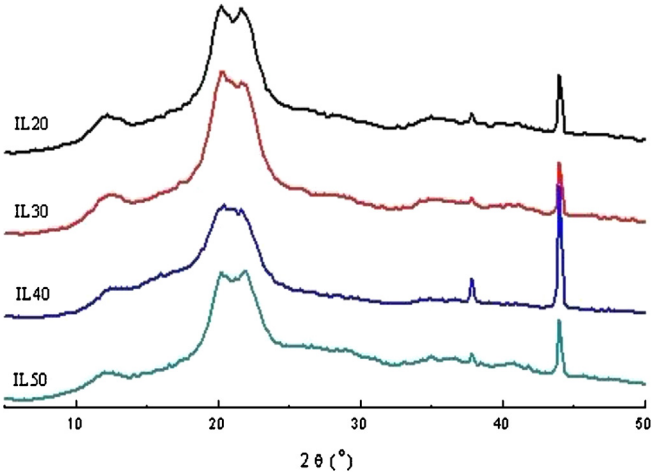


**Fig. 2.** XRD patterns of the regenerated cellulose samples IL20, IL30, IL40, and IL50.

than cellulose I, which facilitates the enzymatic reaction (Cheng et al., 2011).

The crystallinity of the lignocellulosic material has been regarded as a major factor that influences enzymatic hydrolysis. XRD has long been used to determine the crystallinity index by assessing the relative contributions of crystalline fractions to the overall scattering pattern. The CrI of the original cellulose is calculated to be 45.3–47.5%. The pretreatment with [Emim]Ac resulted in a decrease in the crystallinity index to 30.5–34.9%. The lower crystallinity index revealed that a large amount of amorphous cellulose was present in the regenerated cellulose. Highly crystalline cellulose, with a strong interchain hydrogen-bonding network, leads to a high resistance to enzymatic hydrolysis, whereas amorphous cellulose provides a larger surface area accessible by cellulose enzymes and thus it is readily digestible (Yoon, Ang, Ngoh, & Chua, 2012).

### 3.3. FT-IR spectra

FT-IR spectroscopy was applied to compare the molecular conformation changes of the original cellulose after the regeneration. Fig. 3 illustrates the FT-IR spectra of the regenerated cellulose preparations IL20, IL30, IL40, and IL50. All the spectra displayed a common characteristic of cellulose. The absorption of O—H stretching vibration shift from 3340 $cm^{-1}$ of the original cellulose (data not shown) to 3379 $cm^{-1}$ of the regenerated cellulose, indicating the content of the free hydroxyl group increased in the regenerated cellulose (Zhang & Lynd, 2004). The peak at 2897 $cm^{-1}$ is due to the C—H stretching in $CH_2$ and $CH_3$ groups, which is unaffected by changes of crystallinity. The absorption band at 1427 $cm^{-1}$ of the original cellulose is attributed to crystallized cellulose I and amorphous cellulose. This band shifted to 1419 $cm^{-1}$ of the regenerated cellulose, which is characteristic for cellulose II and amorphous cellulose (Carrillo, Colom, Suñol, & Saurina, 2004). The signals at 1365, 1335, and 1277 $cm^{-1}$, represent C—H bending and O—H in-plain deformation, indicating an overwhelming presence of crystalline cellulose II (Široký, Blackburn, Bechtold, Taylor, & White, 2009). The detected band at 1103 $cm^{-1}$ in the original cellulose was not found in the regenerated cellulose, which also revealed a predominance of crystalline cellulose II. The small sharp band at 895 $cm^{-1}$ corresponds to the glycosidic C1—H deformation with ring vibration contribution, which is a characteristic of $\beta$-glycosidic linkages between glucose in cellulose (Pappas, Tarantilis, Daliani, Mavromoustakos, & Polissiou, 2002). The intensity of the regenerated cellulose band is relatively stronger than that of the original cellulose. It has been reported that the intensity of this peak increases with a decrease in the crystallinity of the cellulose sample and a change in the crystal lattice from cellulose I to cellulose II (Nelson & O'Connor, 1964). These observations indicated that the regenerated cellulose has lower crystallinity, and the pretreatment with [Emim]Ac led to the conversion of the crystalline structure of the original cellulose from cellulose I to cellulose II, in well agreement with the results from the X-ray diffraction.

### 3.4. CP/MAS $^{13}C$ NMR spectra

The CP/MAS $^{13}C$ solid-state spectra of the regenerated cellulose IL30 and IL50 are shown in Fig. 4. There are differences between spectra of regenerated cellulose and that of original cellulose. As seen from the CP/MAS $^{13}C$ NMR spectra of the original cellulose, all the noticeable signals of the original cellulose are distributed in the region between 58 and 110 ppm. At the upfield part of the spectra, the region between 60 and 67 ppm is assigned to C6 of the primary alcohol group. The cluster of resonances, between 69 and 81 ppm is attributed to C2, C3 and C5, the ring carbons other than those anchoring the glycosidic linkage. The region between 80 and 90 ppm is associated with C4 and that between 102 and 107 ppm with C1, the anomeric carbon (Atalla & Vanderhart, 1999). In particular, with respect to C-4, the region between 86 and 90 ppm correspond to crystalline forms and para-crystalline of cellulose, whereas the signals in more disordered regions are distributed in a broader band ranging from 80 to 86 ppm. The sharper resonance in the region of C6, centered at 64.39 ppm is assigned to crystalline cellulose, while the broader wings centered at 62.26 ppm arise from amorphous cellulose. In the present study, changes of the regenerated cellulose included the disappearance of the resonance at 64.39 ppm for C-6 of crystalline cellulose, the splitting of the resonances of C4 and C1 in the spectra, and the loss of resolution between C2, C3, and C5 peaks. The disappearance of the resonance in the crystalline area clearly showed a decrease in CrI, i.e., increase in the proportion of amorphous regions. This phenomenon, consistent with the XRD and FT-IR analysis, suggested that cellulose re-crystallized in a lattice similar to that of cellulose II after [Emim]Ac dissolution (Atalla & Vanderhart, 1999).

### 3.5. Scanning electron microscopy images

Fig. 5 shows the SEM images of the regenerated cellulose IL40 under various magnifications as compared to the original cellulose. There was apparent difference in the morphology of the original cellulose and regenerated cellulose under lower magnification (300×). The original cellulose had a long and well-separated macrofibrils whereas the cellulose is observed to be fused and agglomerated after [Emim]Ac treatment (Fig. 5(a)). Magnified images (3000×, 5000× and 10 000×) revealed that the surfaces of the untreated fibers were smooth and the pretreated cellulose presented rougher surfaces and more porosity (Fig. 5(b)–(d)). These alterations may be attributed to the disruption of the structure and reduction in crystallinity. Accessibility of the substrate to the cellulolytic enzymes is one of the major factors influencing the hydrolysis process. Previous study has illustrated that the cellulases can get trapped in the pores if the internal area is much larger than the external area (Zhang & Lynd, 2004). Thus, one of the objectives of the pretreatment is to increase the porosity and available surface area for the enzymatic attack (Alvira, Tomas-Pejo, Ballesteros, & Negro, 2010). The morphological investigation in the present study showed a significant increase in the porosity and surface area after the pretreatment, thus contribute to the enhancement of subsequent enzymatic hydrolysis.

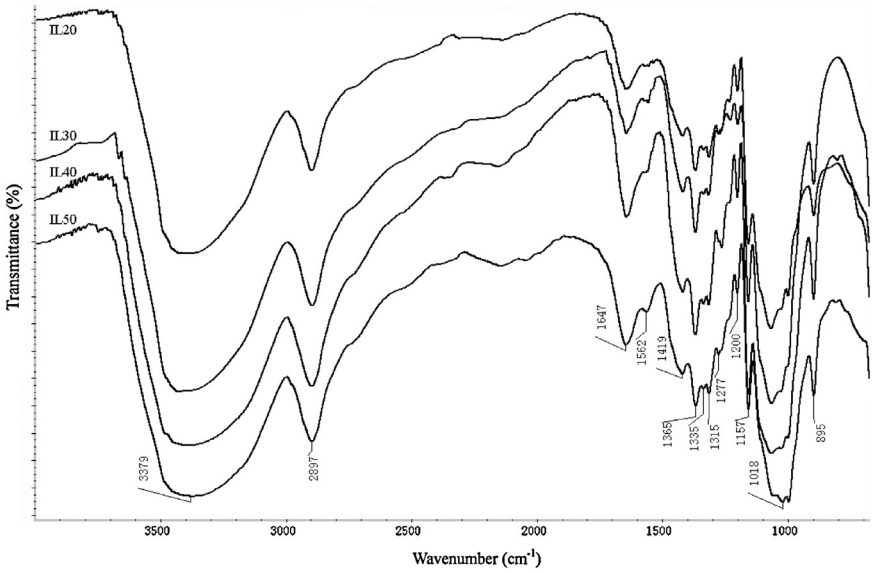


**Fig. 3.** FT-IR spectra of the regenerated cellulose samples IL20, IL30, IL40, and IL50.

### 3.6. *Effect of structural changes on the enzymatic hydrolysis*

The structural modifications of the cellulose are highly dependent on the type of pretreatment employed and have great effects on the enzymatic hydrolysis (Kumar & Wyman, 2009). The digestibility of the cellulose was examined by enzymatic hydrolysis with a mixture of cellulase and β-glucosidase. Fig. 6 shows the time course of original cellulose C30 and regenerated cellulose IL30. The conversion is defined as the percentage of glucose released in the hydrolysate divided by the potential glucose in the cellulose sample. As can be seen, the conversion of both the original and regenerated cellulose increased with the increase of

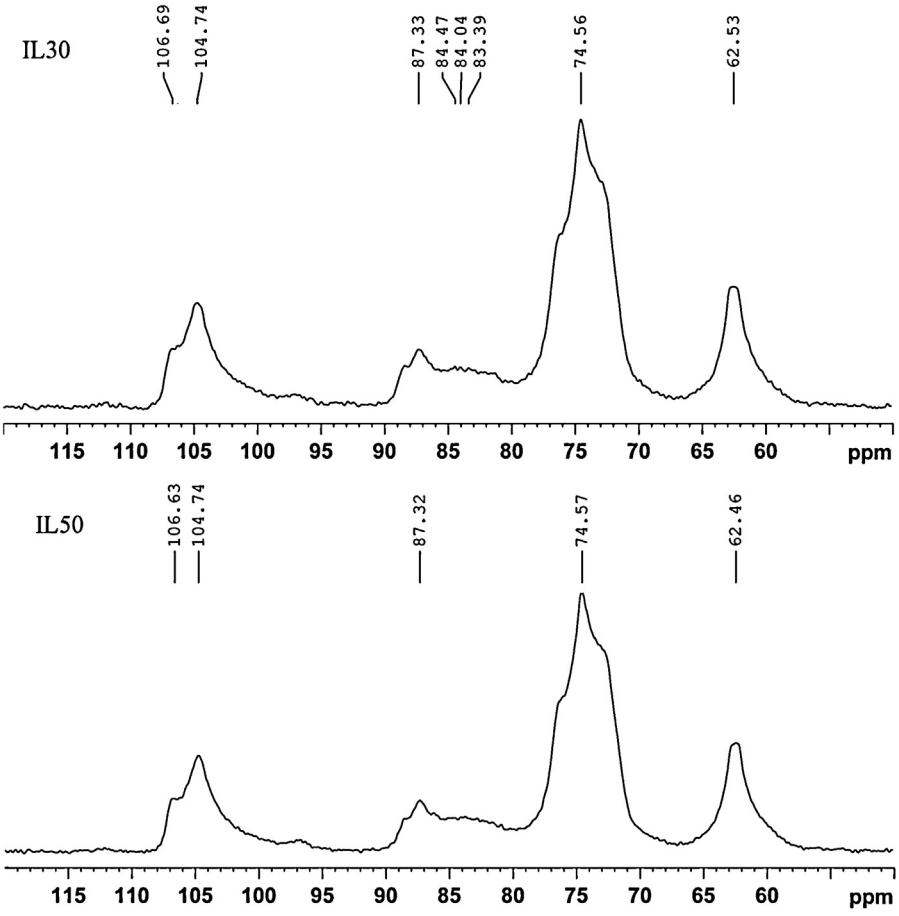


**Fig. 4.** CP/MAS $^{13}C$ NMR spectra of the regenerated cellulose samples IL30 and IL50.

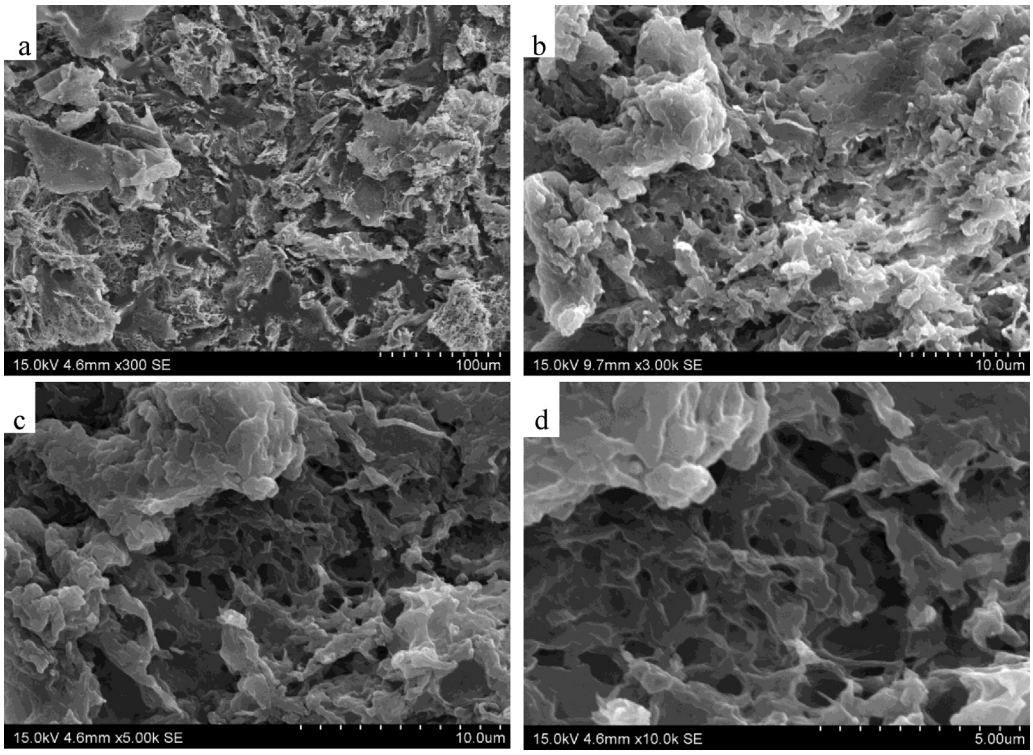


**Fig. 5.** SEM images at various magnifications of the regenerated cellulose IL40. (a) IL40 at 300×, (b) IL40 at 3000×, (c) IL40 at 5000×, and (d) IL40 at 10 000×.

the hydrolysis time. The regenerated cellulose was converted into glucose by 39.5% after 6 h, whereas the conversion yield of original cellulose C30 was 26.4% after 6 h hydrolysis. The conversion of original cellulose C30 was 64.1% and 84.9% for 48 h and 96 h, respectively. For regenerated cellulose, a high conversion of 95.2% was achieved after 96 h. This cellulose digestibility is higher than that of the sample subjected to a combination treatment with ionic liquid 1-butyl-3-methylimidazolium methylsulfate and $H_2SO_4$, which led a cellulose digestibility of 77% at the optimum pretreatment condition (Diedericks, Rensburg, García-Aparicio, & Görgens, 2012). Obviously, the regenerated cellulose exhibited higher glucose conversion rate and yield than the original cellulose. The phenomenon suggested that IL [Emim]Ac pretreatment provided an effective process to enhance the conversion of cellulose to glucose. This is consistent with the results reported by Silva, Lee, Endo, and Bon (2011), who have also found that [Emim]Ac was the most efficient IL among the six ILs used as it significantly enhanced bagasse enzymatic saccharification rate and yield.

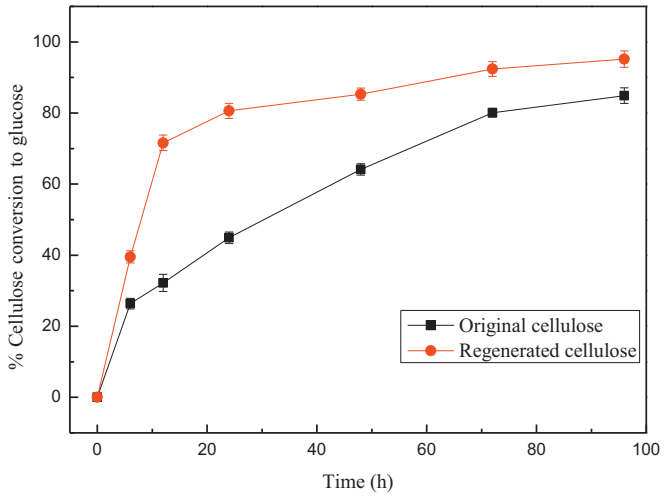


**Fig. 6.** Enzymatic hydrolysis of original cellulose C30 and regenerated cellulose IL30.

In general, the enhancement would mainly be ascribed to the structural changes as determined in the present study, such as the degree of polymerization of cellulose, cellulose crystallinity, cellulose crystal structure, and the porosity and surface area of the cellulose. Both DP and crystallinity of cellulose were inversely related to the enzymatic hydrolysis yield. The lower DP represents the existence of a higher amount of reducing ends that will provide more sites for cellulase to initiate the cleavage of cellulose (Zhang & Lynd, 2004). Furthermore, shorter chains allow cellulose to be more prone to enzymatic deconstruction since they form weaker networks fostering enzyme access (Monrroy, Ortega, Ramirez, Baeza, & Freer, 2011). Therefore, the lower DP of the regenerated cellulose improved the enzymatic hydrolysis. In the highly ordered region, cellulose chains are tightly packed, resulting in the limited accessibility of cellulose to swelling and reactive agents such as cellulase. On the contrary, amorphous cellulose has more accessibility to the reaction. Therefore, a decrease of the crystallinity enhanced the enzymatic hydrolysis of cellulose. Uju et al. (2012) reported that the increase in the reaction rates with [Emim]Ac treatment was mainly because of a reduction in the cellulose crystallinity, and those with 1-buthyl-3-methylpyridinium chloride treatment was due to a reduction in the degree of polymerization of cellulose. However, we found that the [Emim]Ac treatment caused both the reduction of crystallinity and the degree of polymerization, which led to the enhancement of the cellulose conversion. In this study, the crystal structure of cellulose transformed from cellulose I to cellulose II after IL [Emim]Ac pretreatment. This may be another important feature that affects the enzymatic hydrolysis. The cellulose I of the original cellulose consists of parallel chains forming hydrogen-bonded sheet that stack through hydrophobic interaction such as van der Waals force, and there is no hydrogen bonding between the sheets. In cellulose II of the regenerated cellulose, antiparallel chains are stacked through

hydrophobic interaction and further stabilizing with intermolecular hydrogen bonds (Wada et al., 2010). It has been reported that smaller *d*-spacing indicates stronger hydrophobic interaction and cellulose I has smaller *d*-spacing than cellulose II (Wada, Chanzy, Nishiyama, & Langan, 2004). Hydrophobic interactions between the molecular chains would act as a main factor to resist enzymatic hydrolysis by cellulase, while hydrogen bonds in the first layer of cellulose crystallites could become unstable in water (Wada et al., 2010). Therefore, the much weaker hydrophobic interaction in cellulose II than that in cellulose I could be one of the most important reasons for the large enhancement of enzymatic hydrolysis. In addition, the accessibility of cellulose to the limited adsorption sites on crystalline cellulose is generally believed to play an important role in cellulose hydrolysis. After IL pretreatment, the cellulose became more porous and had more surface area accessible to cellulases adsorption, which increased enzymatic accessibility. This was in good agreement with the previous report that the ability of IL facilitates the mass transport of enzymes to the cellulose surface, resulting in improved cellulose enzymatic saccharification (Silva et al., 2011).

## 4. Conclusions

Ionic liquid [Emim]Ac was used to dissolve the original cellulose isolated from sugarcane bagasse. After being regenerated form IL, cellulose experienced an increase in glucose content, a decrease in the degree of polymerization and crystallinity index, a transformation of cellulose crystal from cellulose I to cellulose II, and an increase in surface area. The enzymatic hydrolysis rate and yield of the regenerated cellulose for the production of glucose was largely enhanced, indicating that the changes of cellulose are significant in relation to the enzymatic hydrolysis. Although the findings primarily confirm the relationship between the structural changes and enzymatic hydrolysis, further work is required to specify more precisely the relationship between cellulose structure and digestibility.

## Acknowledgments

The authors are grateful to grants from the Fundamental Research Funds for the Central Universities (BLYJ201215), Natural Science Foundation of China (No. 30930073), the Ministry of Science and Technology (973, 2010CB732204), and China Ministry of Education (No. 111).

## References

Alvira, P., Tomas-Pejo, E., Ballesteros, M., & Negro, M. J. (2010). Pretreatment technologies for an efficient bioethanol production process based on enzymatic hydrolysis: A review. *Bioresource Technology*, *101*, 4851–4861.

Arantes, V., & Saddler, J. N. (2011). Cellulose accessibility limits the effectiveness of minimum cellulase loading on the efficient hydrolysis of pretreated lignocellulosic substrates. *Biotechnology for Biofuels*, *4*, 3.

Atalla, R. H., & Vanderhart, D. L. (1999). The role of solid state $^{13}C$ NMR spectroscopy in studies of the nature of native celluloses. *Solid State Nuclear Magnetic Resonance*, *15*, 1–19.

Azubuike, C. P., Rodríguez, H., Okhamafe, A. O., & Rogers, R. D. (2011). Physicochemical properties of maize cob cellulose powders reconstituted from ionic liquid solution. *Cellulose*, *19*, 425–433.

Bian, J., Peng, F., Peng, X. P., Peng, P., Xu, F., & Sun, R. C. (2012). Acetic acid enhanced purification of crude cellulose from sugarcane bagasse: Structural and morphological characterization. *Bioresources*, *7*, 4626–4639.

Carrillo, F., Colom, X., Suñol, J. J., & Saurina, J. (2004). Structural FTIR analysis and thermal characterisation of lyocell and viscose-type fibres. *European Polymer Journal*, *40*, 2229–2234.

Cateto, C., Hu, G., & Ragauskas, A. (2011). Enzymatic hydrolysis of organosolv Kanlow switchgrass and its impact on cellulose crystallinity and degree of polymerization. *Energy & Environmental Science*, *4*, 1516–1521.

Chang, V. S., & Holtzapple, M. T. (2000). Fundamental factors affecting biomass enzymatic reactivity. *Applied Biochemistry Biotechnology*, *84–86*, 5–37.

Cheng, G., Varanasi, P., Li, C., Liu, H., Melnichenko, Y. B., Simmons, B. A., et al. (2011). Transition of cellulose crystalline structure and surface morphology of biomass as a function of ionic liquid pretreatment and its relation to enzymatic hydrolysis. *Biomacromolecules*, *12*, 933–941.

Dadi, A. P., Schall, C. A., & Varanasi, S. (2007). Mitigation of cellulose recalcitrance to enzymatic hydrolysis by ionic liquid pretreatment. *Applied Biochemistry and Biotechnology*, 407–421.

Diedericks, D., Rensburg, E., García-Aparicio, M. P., & Görgens, J. F. (2012). Enhancing the enzymatic digestibility of sugarcane bagasse through the application of an ionic liquid in combination with an acid catalyst. *Biotechnology Progress*, *28*, 76–84.

Duchesne, I., Hult, E., Molin, U., Daniel, G., Iversen, T., & Lennholm, H. (2001). The influence of hemicellulose on fibril aggregation of kraft pulp fibres as revealed by FE-SEM and CP/MAS $^{13}C$ NMR. *Cellulose*, *8*, 103–111.

Farrell, A. E., Plevin, R. J., Turner, B. T., Jones, A. D., O'hare, M., & Kammen, D. M. (2006). Ethanol can contribute to energy and environmental goals. *Science*, *311*, 506–508.

Kumar, R., & Wyman, C. E. (2009). Does change in accessibility with conversion depend on both the substrate and pretreatment technology? *Bioresource Technology*, *100*, 4193–4202.

Kuo, C. H., & Lee, C. K. (2009). Enhancement of enzymatic saccharification of cellulose by cellulose dissolution pretreatments. *Carbohydrate Polymers*, *77*, 41–46.

Lee, S. H., Doherty, T. V., Linhardt, R. J., & Dordick, J. S. (2009). Ionic liquid-mediated selective extraction of lignin from wood leading to enhanced enzymatic cellulose hydrolysis. *Biotechnology and Bioengineering*, *102*, 1368–1376.

Liebert, T. (2010). Cellulose solvents – remarkable history, bright future. In T. F. Liebert, T. J. Heinze, & K. J. Edgar (Eds.), *Cellulose solvents: For analysis, shaping and chemical modification* (pp. 3–54). New York: Oxford University Press.

Monrroy, M., Ortega, I., Ramirez, M., Baeza, J., & Freer, J. (2011). Structural change in wood by brown rot fungi and effect on enzymatic hydrolysis. *Enzyme and Microbial Technology*, *49*, 472–477.

Nelson, M. L., & O'Connor, R. T. (1964). Relation of certain infrared bands to cellulose crystallinity and crystal lattice type. Part II. A new infrared ratio for estimation of crystallinity in celluloses I and II. *Journal of Applied Polymer Science*, *8*, 1325–1341.

Nishiyama, Y., Sugiyama, J., Chanzy, H., & Langan, P. (2003). Crystal structure and hydrogen bonding system in cellulose Iα from synchrotron X-ray and neutron fiber diffraction. *Journal of the American Chemical Society*, *125*, 14300–14306.

Pandey, A., Soccol, C. R., Nigam, P., Soccol, V. T., Vandenberghe, L. P. S., & Mohan, R. (2000). Biotechnological potential of agro-industrial residues. II: Cassava bagasse. *Bioresource Technology*, *74*, 81–87.

Pappas, C., Tarantilis, P., Daliani, I., Mavromoustakos, T., & Polissiou, M. (2002). Comparison of classical and ultrasound-assisted isolation procedures of cellulose from kenaf (*Hibiscus cannabinus L.*) and eucalyptus (*Eucalyptus rodustrus Sm.*). *Ultrasonics Sonochemistry*, *9*, 19–23.

Pinkert, A., Marsh, K. N., Pang, S., & Staiger, M. P. (2009). Ionic liquids and their interaction with cellulose. *Chemical Reviews*, *109*, 6712–6728.

Richard, T. L. (2010). Challenges in scaling up biofuels infrastructure. *Science*, *329*, 793–796.

Silva, A. S., Lee, S. H., Endo, T., & Bon, E. P. (2011). Major improvement in the rate and yield of enzymatic saccharification of sugarcane bagasse via pretreatment with the ionic liquid 1-ethyl-3-methylimidazolium acetate ([Emim][Ac]). *Bioresource Technology*, *102*, 10505–10509.

Segal, L., Creely, J., Martin, A., Jr., & Conrad, C. (1959). An empirical method for estimating the degree of crystallinity of native cellulose using the X-ray diffractometer. *Textile Research Journal*, *29*, 786–794.

Široký, J., Blackburn, R. S., Bechtold, T., Taylor, J., & White, P. (2009). Attenuated total reflectance Fourier-transform Infrared spectroscopy analysis of crystallinity changes in lyocell following continuous treatment with sodium hydroxide. *Cellulose*, *17*, 103–115.

Sun, N., Rahman, M., Qin, Y., Maxim, M. L., Rodríguez, H., & Rogers, R. D. (2009). Complete dissolution and partial delignification of wood in the ionic liquid 1-ethyl-3-methylimidazolium acetate. *Green Chemistry*, *11*, 646–655.

Uju, ShodaY., Nakamoto, A., Goto, M., Tokuhara, W., Noritake, Y., Katahira, S., et al. (2012). Short time ionic liquids pretreatment on lignocellulosic biomass to enhance enzymatic saccharification. *Bioresource Technology*, *103*, 446–452.

Wada, M., Chanzy, H., Nishiyama, Y., & Langan, P. (2004). Cellulose $III_1$ crystal structure and hydrogen bonding by synchrotron X-ray and neutron fiber diffraction. *Macromolecules*, *37*, 8548–8555.

Wada, M., Ike, M., & Tokuyasu, K. (2010). Enzymatic hydrolysis of cellulose I is greatly accelerated via its conversion to the cellulose II hydrate form. *Polymer Degradation and Stability*, *95*, 543–548.

Wang, K., Jiang, J. X., Xu, F., & Sun, R. C. (2009). Influence of steaming explosion time on the physic-chemical properties of cellulose from *Lespedeza* stalks (*Lespedeza crytobotrya*). *Bioresource Technology*, *100*, 5288–5294.

Yoon, L. W., Ang, T. N., Ngoh, G. C., & Chua, A. S. M. (2012). Regression analysis on ionic liquid pretreatment of sugarcane bagasse and assessment of structural changes. *Biomass and Bioenergy*, *36*, 160–169.

Zavrel, M., Bross, D., Funke, M., Büchs, J., & Spiess, A. C. (2009). High-throughput screening for ionic liquids dissolving (ligno-) cellulose. *Bioresource Technology*, *100*, 2580–2587.

Zhang, Y. H., & Lynd, L. R. (2004). Toward an aggregated understanding of enzymatic hydrolysis of cellulose: Noncomplexed cellulase systems. *Biotechnology and Bioengineering*, *88*, 797–824.

Zuluaga, R., Putaux, J. L., Cruz, J., Vélez, J., Mondragon, I., & Gaṇán, P. (2009). Cellulose microfibrils from banana rachis: Effect of alkaline treatments on structural and morphological features. *Carbohydrate Polymers*, *76*, 51–59.